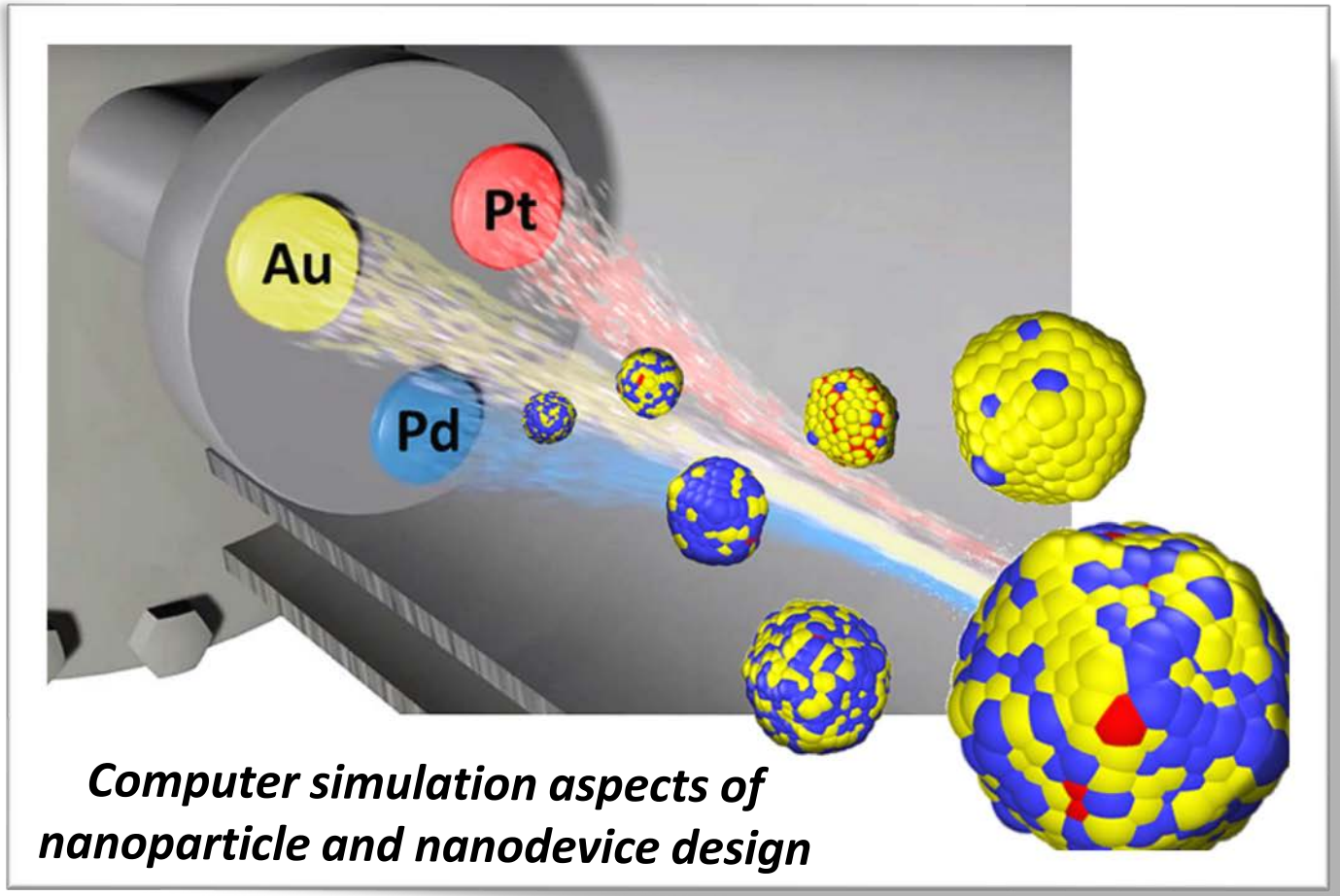

Computer simulation aspects of nanoparticle and nanodevice design

Panagiotis Grammatikopoulos

26 January 2021

OIST's *Nanoparticles by Design* Unit

OIST's *Nanoparticles by Design* Unit

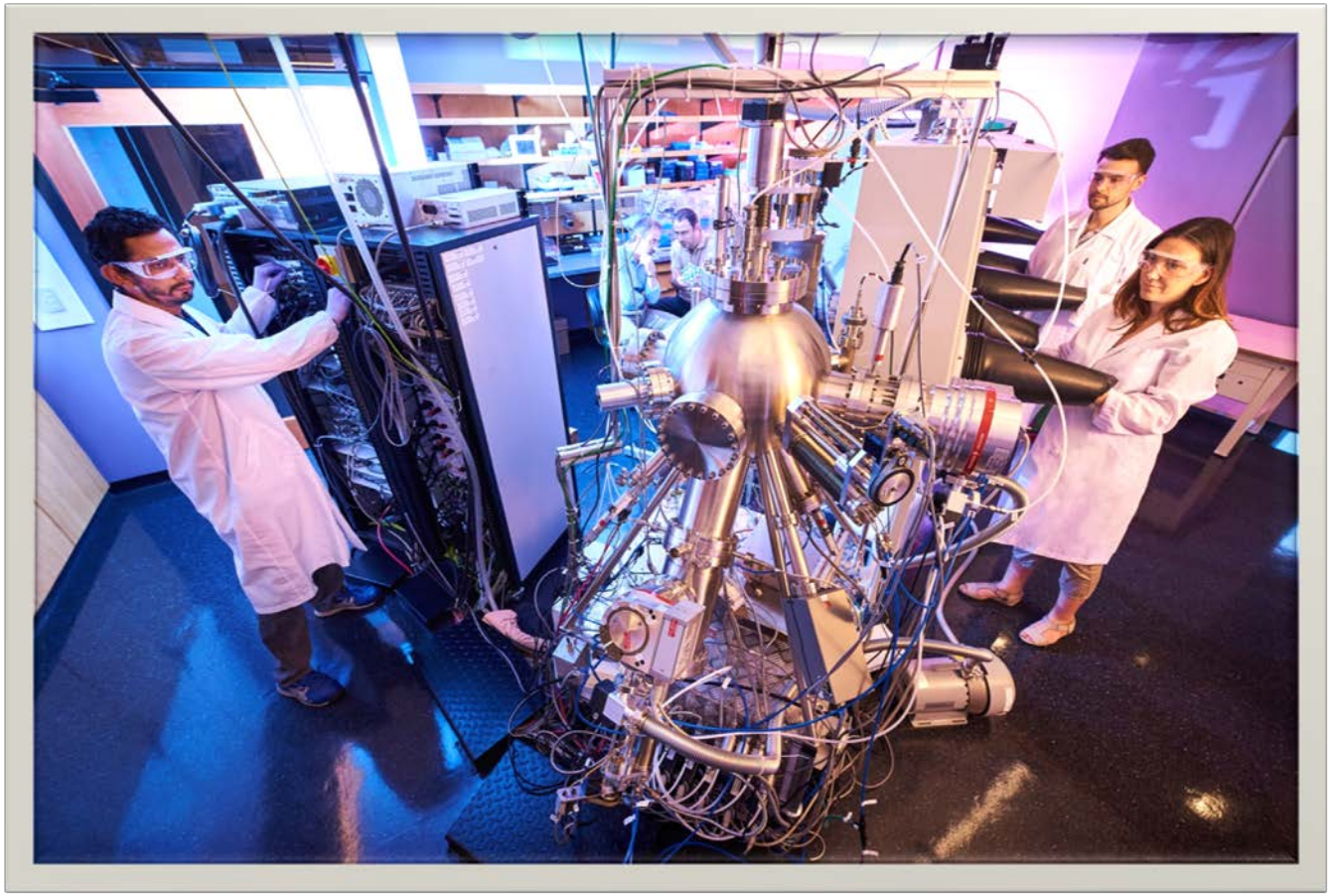

These labs are remarkably diverse – here's why they're winning at science, Nature 2018

Cluster Beam Deposition Sources

using rare gas to produce supersaturated vapours

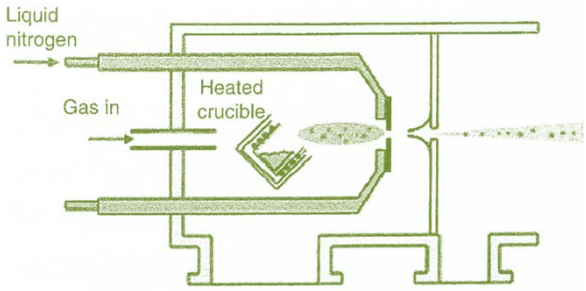

thermal gas aggregation

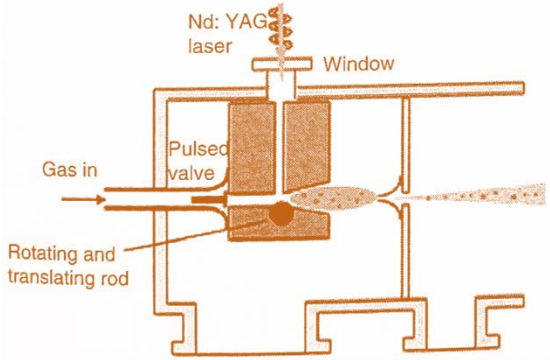

laser ablation

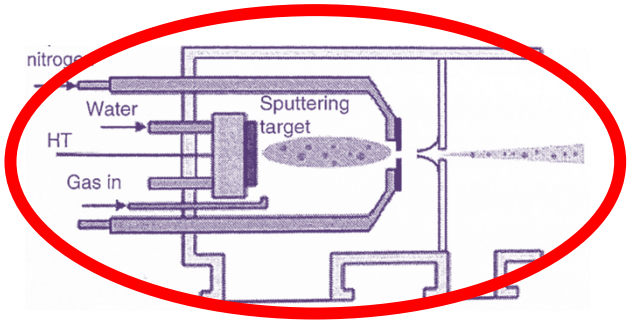

sputter gas aggregation

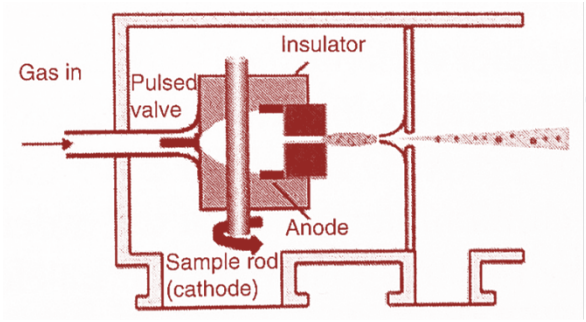

pulsed microplasma

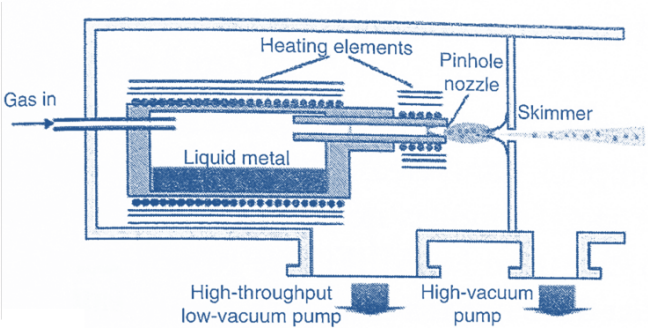

seeded supersonic nozzle

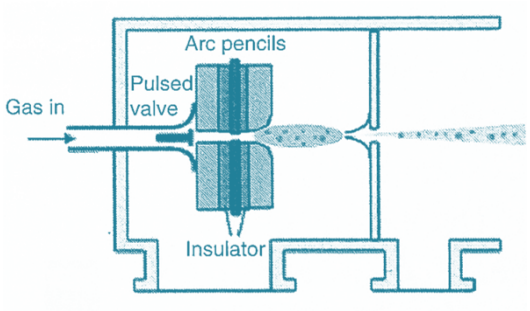

pulsed-arc cluster ion

Gas-Phase Synthesis of Nanoparticles; Huttel, Y., Ed.; Wiley-VCH: Weinheim, 2017.

Magnetron-sputtering inert-gas condensation

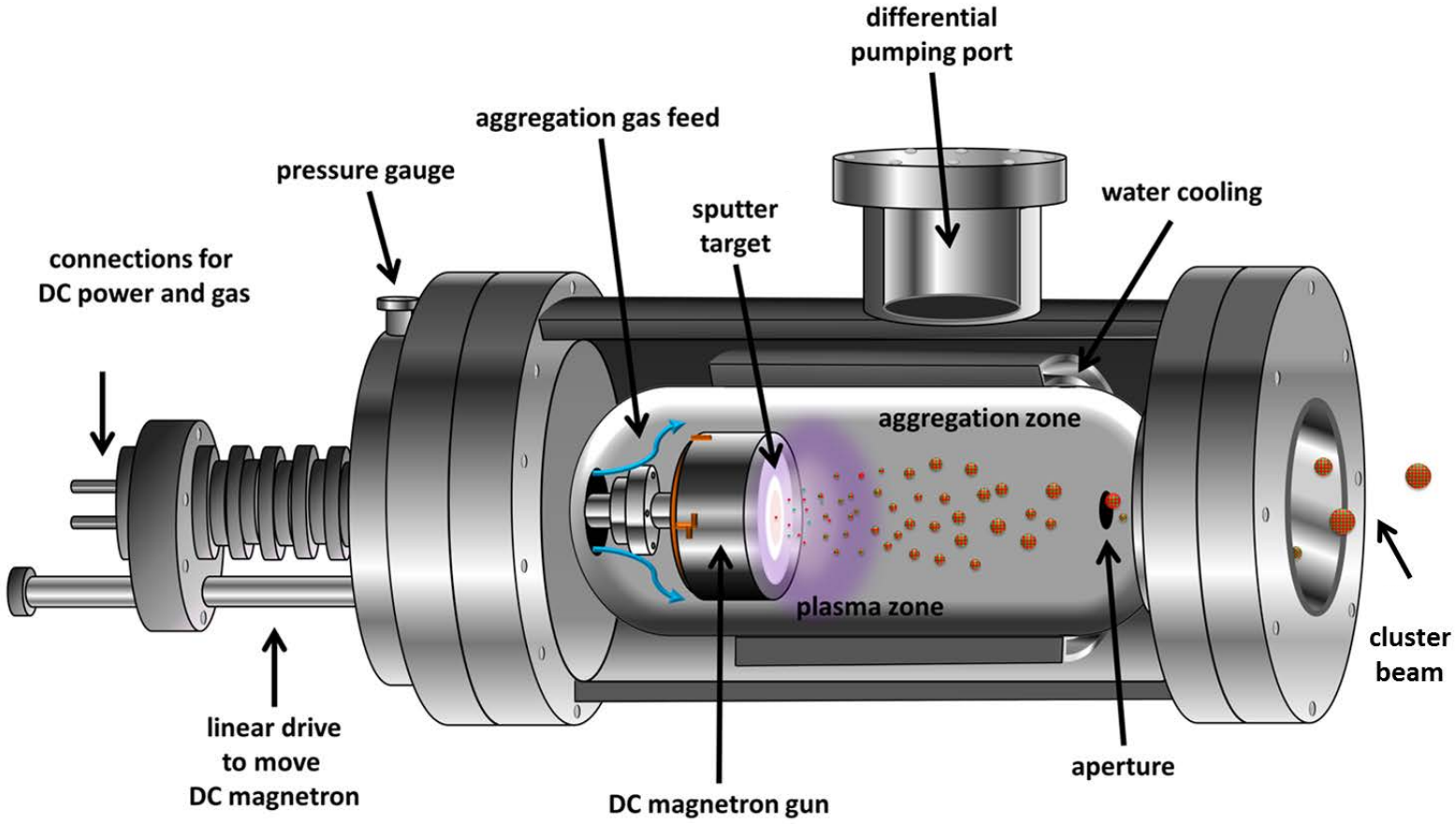

Schematic representation of a DC magnetron-sputtering, inert-gas condensation, cluster beam deposition system, utilizing a single alloy target of the desired composition.

"Tuning the onset of ferromagnetism in heterogeneous bimetallic nanoparticles by gas phase doping"
M. Bohra, P. Grammatikopoulos, V. Singh, J. Zhao, E. Toulkeridou, S. Steinhauer, J. Kioseoglou, J.-F. Bobo, K. Nordlund, F. Djurabekova, M. Sowwan, *Phys Rev Mater* (2017)

Magnetron-sputtering inert-gas condensation

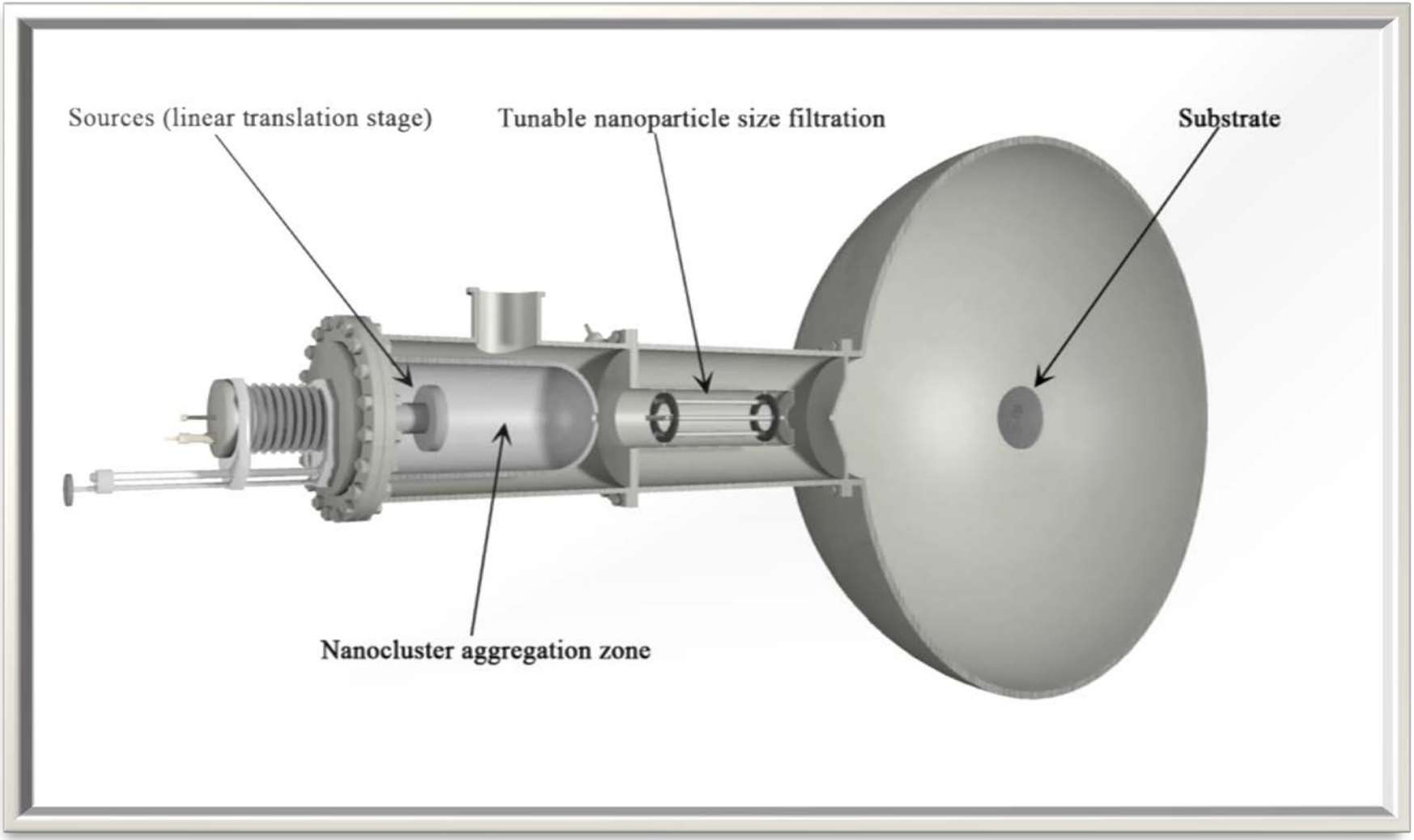

From Nanoparticles by Design…

individual atoms

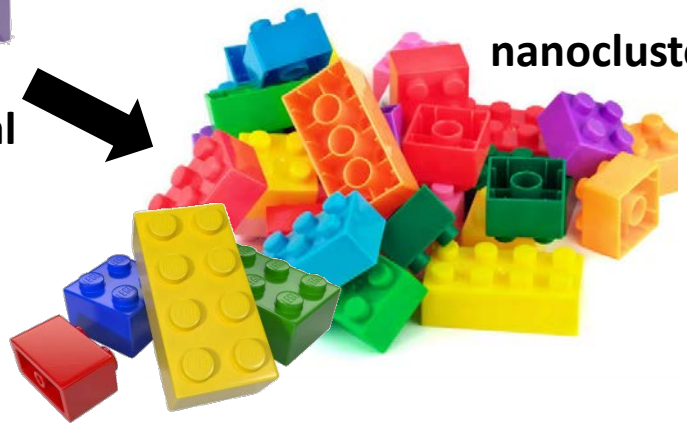

nanoclusters

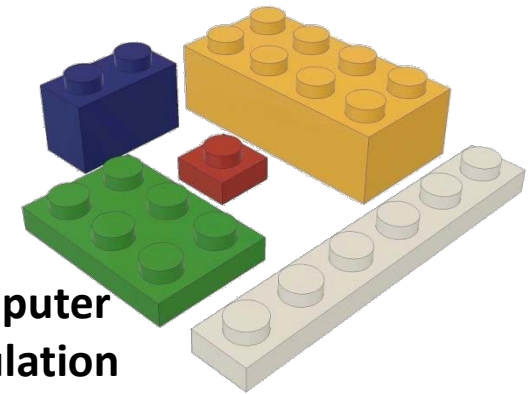

computer simulation

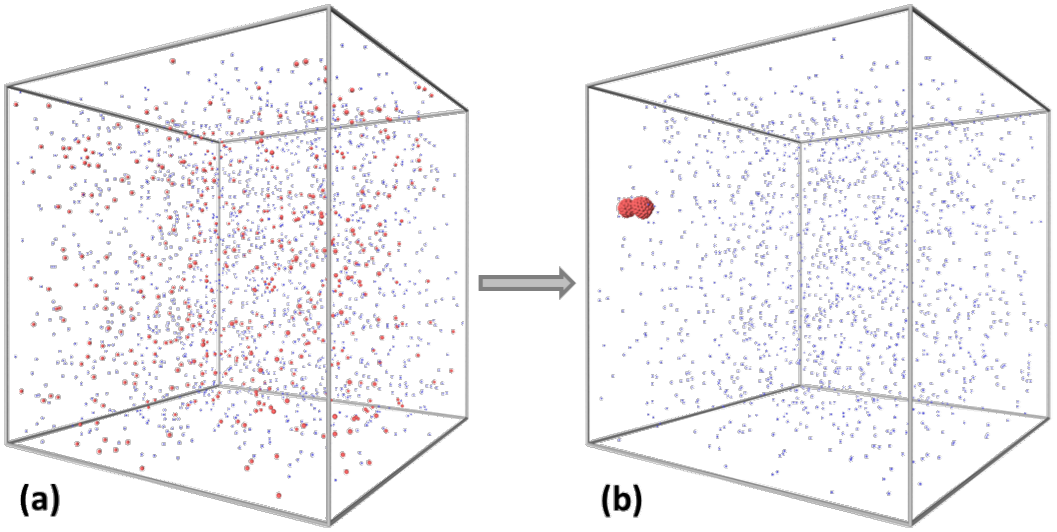

initial configuration

final configuration

MD simulation of Si NP growth:
500 Si (red) and 1500 Ar (blue) atoms.

Temperature and potential energy evolution during growth. The inset zooms in at the initial 2.5 ns of the process. MD simulation snapshots designate various stages of the growth mechanism.

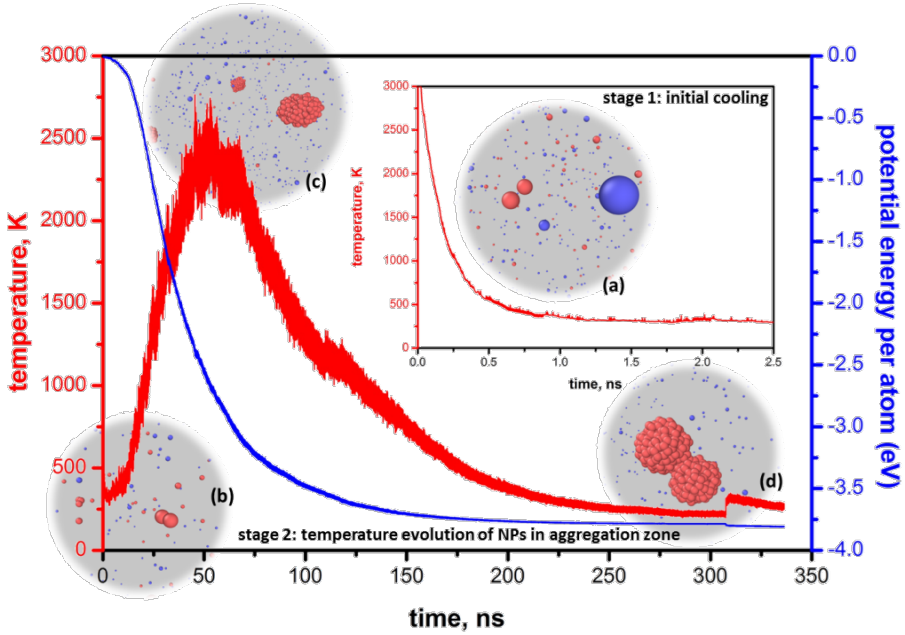

"*Nanoparticle formation via magnetron sputtering with inert gas aggregation*",
chapter 16 of "*Nanostructured semiconductors: amorphisation and thermal properties*"
P. Grammatikopoulos, M. Sowwan
CRC Press, Boca Raton (**2017**), ISBN: 978-9-814-74564-2.

Nanoalloys form via various setups

(i) Two separate targets

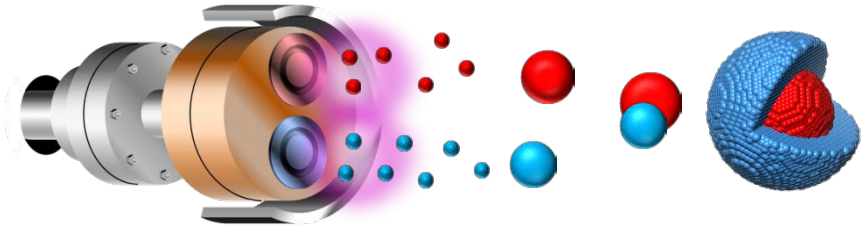

(AgCu, FeAu, FeAl, FePd, AgSi, PdMg, NiPt)

(ii) Post-growth shell coating

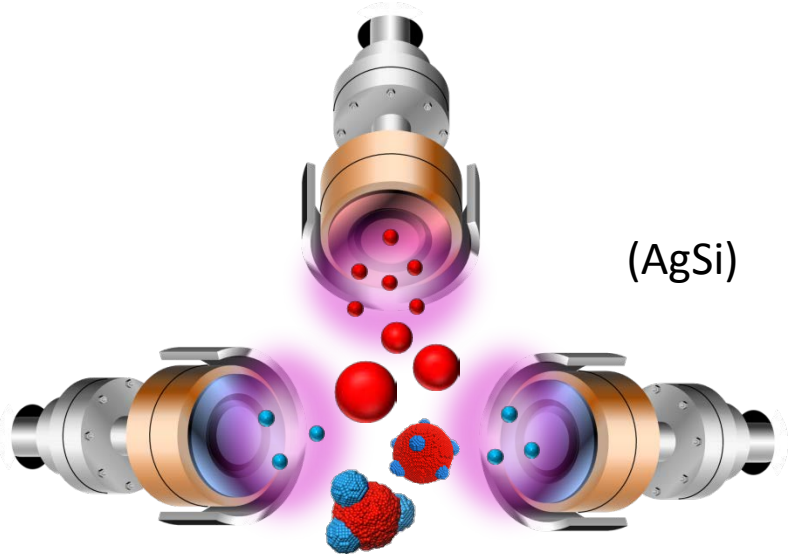

(AgSi)

(iii) One composite target

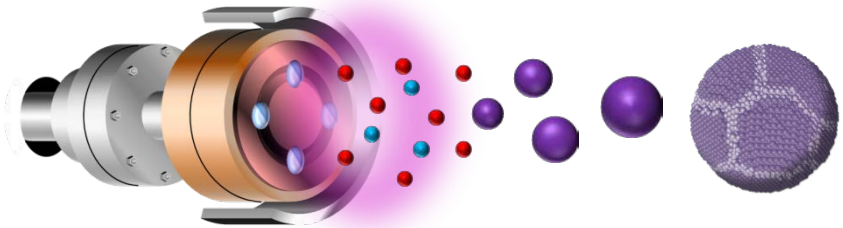

(FeAu)

(iv) One alloy target

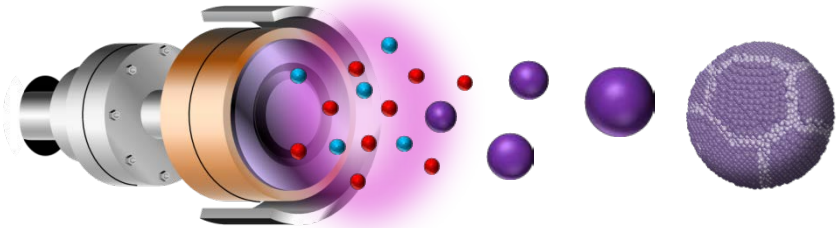

(NiCr)

Nanoalloys form via various setups

(i) Two separate targets

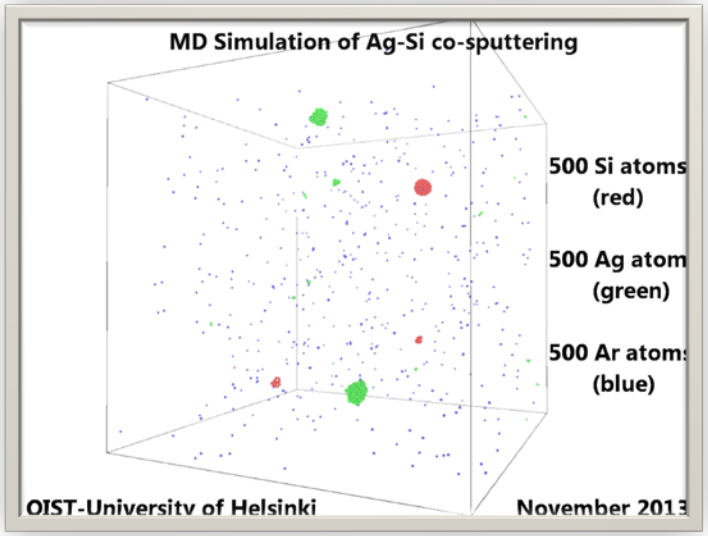

(ii) Post-growth shell coating

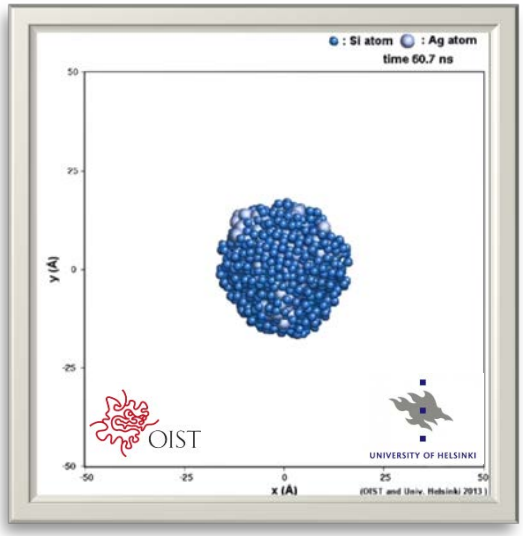

(iii) One composite target

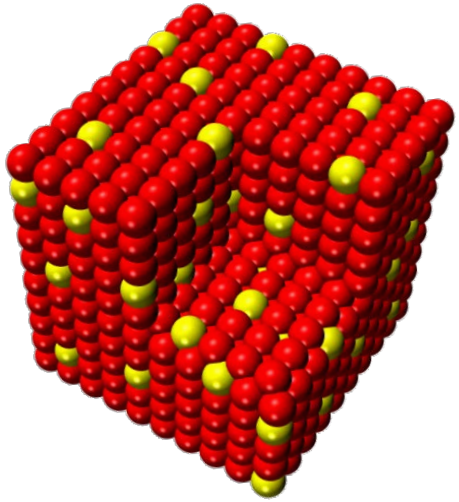

(iv) One alloy target

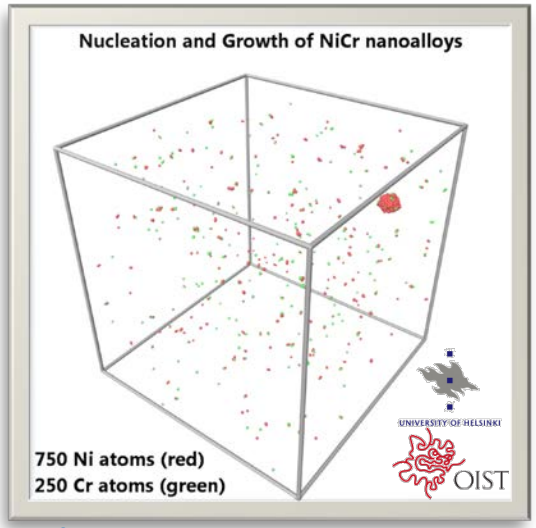

JPC C 118:25 ***(2014)*** *13869* *Sci Rep* 3 **(2013)** 3083 *Adv Funct Mater* 27 **(2017)** 1605328 *Phys Rev Mater* 1 **(2017)** 066001

Nanoalloys form via various setups

(i) Two separate targets

(AgSi)

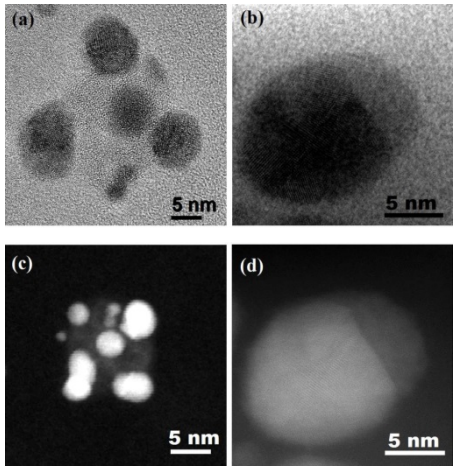

Bright-field HRTEM (a, b) and HAADF–STEM (c, d) image of the core-satellite (a, c) and Janus (b, d) Si-Ag nanoparticles, respectively.

(ii) Post-growth shell coating

(AgSi)

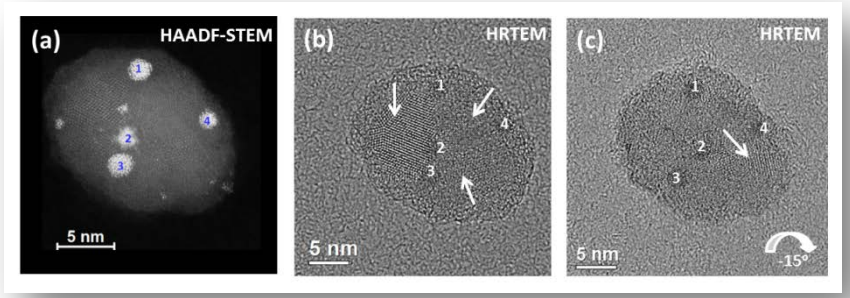

Ag clusters are numbered 1–4 . Three crystal grains are indicated by arrows. (c) A fourth crystal grain is confirmed by tilting the sample by −15◦ relative to the incident electron beam. Qualitative correlation between the number of Ag clusters and the number of grains in the Si core is evident.

(iii) One composite target

(FeAu)

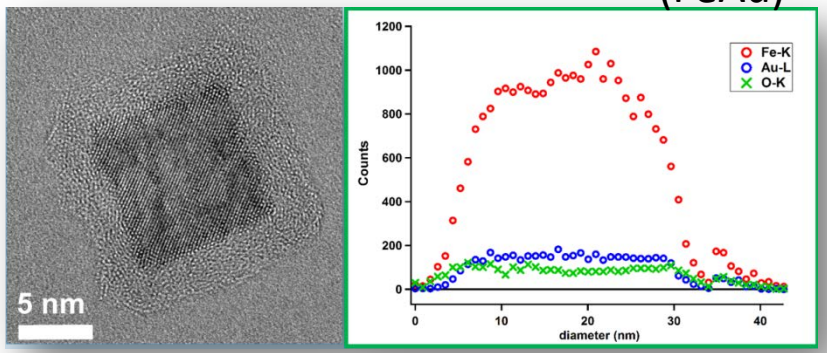

HR-TEM image and EDX linescan profile of a representative single crystalline FeAu nanocube.

(iv) One alloy target

(NiCr)

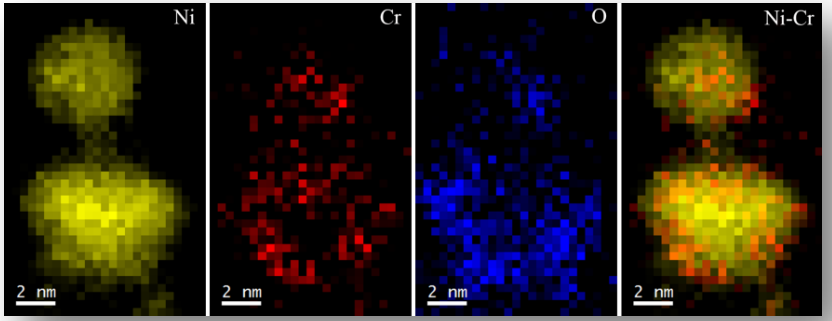

EELS elemental maps of two NCs showing Ni cores and NiCrOx shells. The oxidisation is due to exposure to air during transportation of the sample.

JPC C 118:25 ***(2014)*** *13869* *Sci Rep* 3 **(2013)** 3083 *Adv Funct Mater* 27 **(2017)** 1605328 *Microsc. Microanal. 20* **(2014)** 1664

Nucleation rate varies with element affecting size of clusters and chemical order of nanoalloys

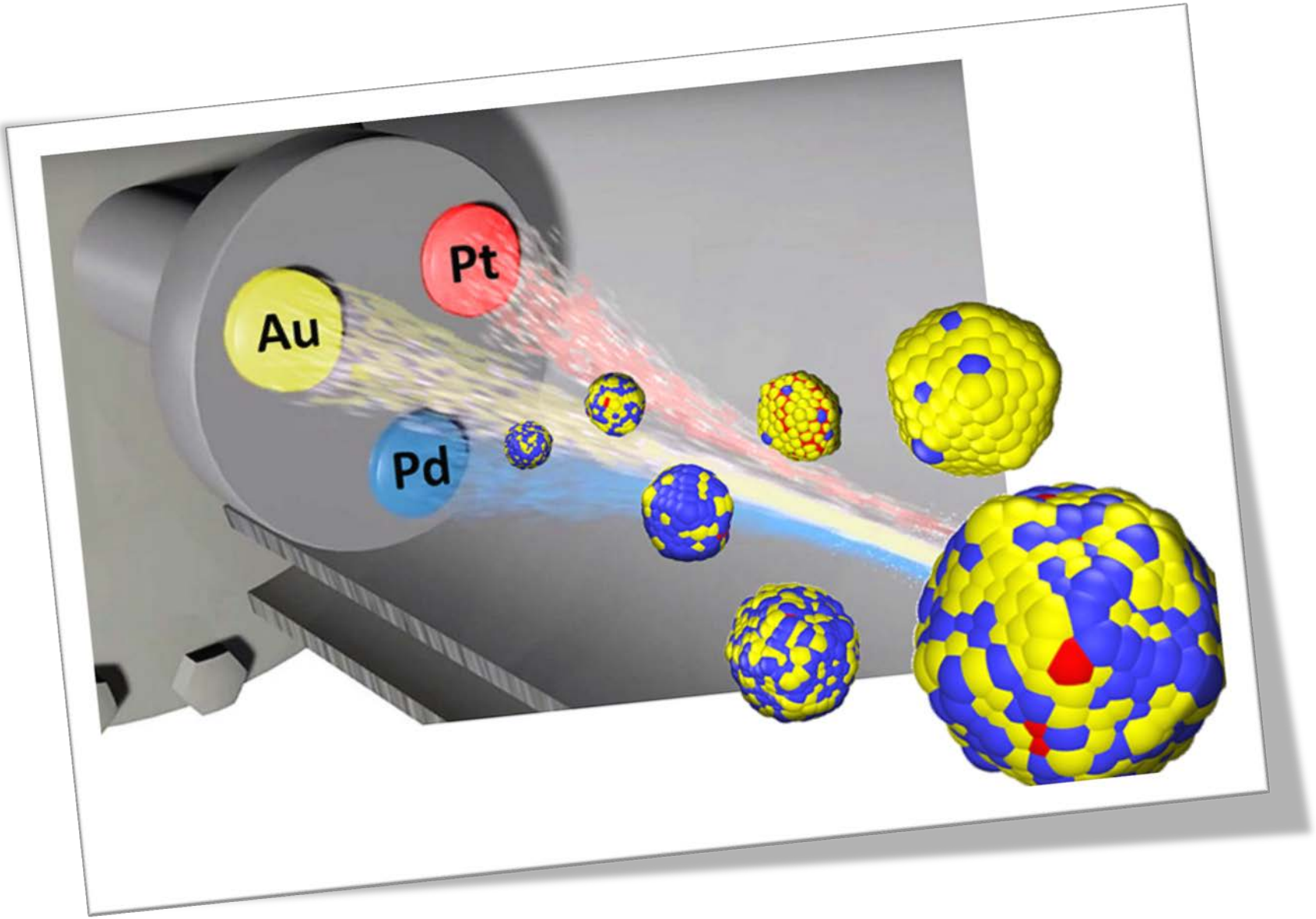

Mattei et al. Chem Mater, 31:6 (2019) 2151-2163

NP nucleation & growth simulation setup

MD growth of trimetallic NPs

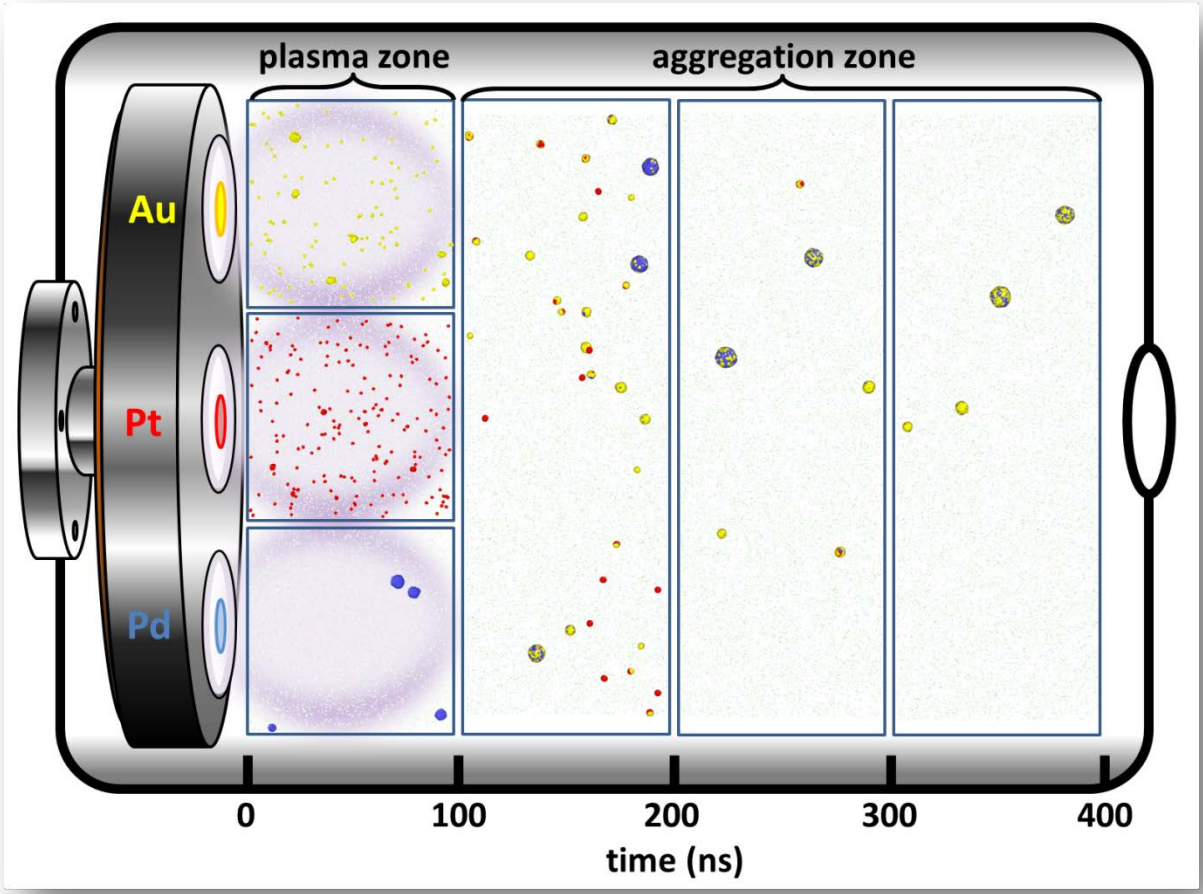

Schematics of MD arrangement - correspondence to experimental setup

Mattei et al. Chem Mater, 31:6 (2019) 2151-2163

Nucleation kinetics

MD growth of monometallic NPs

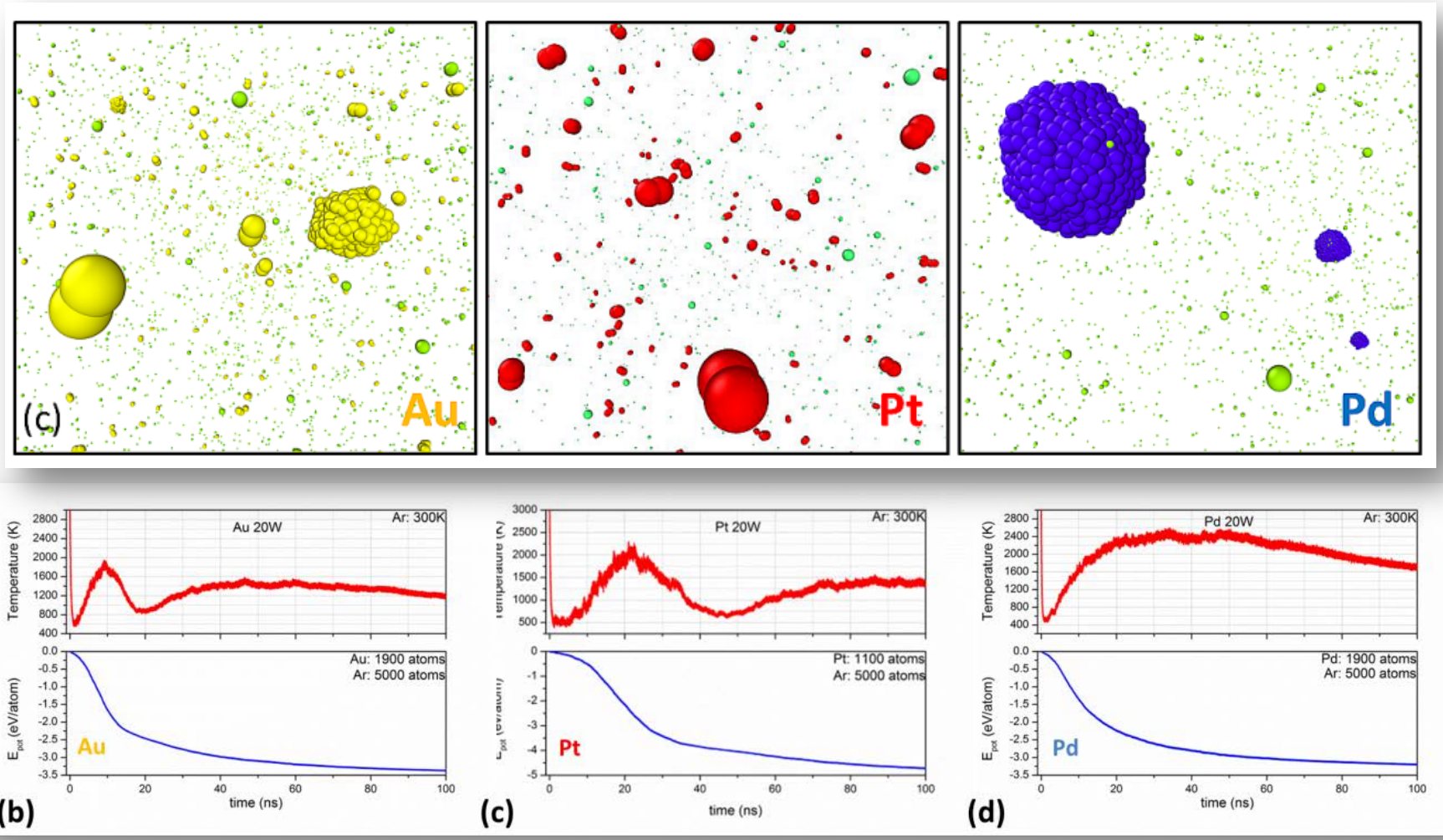

Growth enhanced by low temperature and high magnetron power

Pd NPs form faster than Au or Pt

Temperature spikes for Au and Pt correspond to iucleation of dimers, not immediately followed by further growth

Pd clusters of larger sizes readily form: high and broad temperature peak

Mattei et al. Chem Mater, 31:6 (2019) 2151-2163

Nucleation kinetics

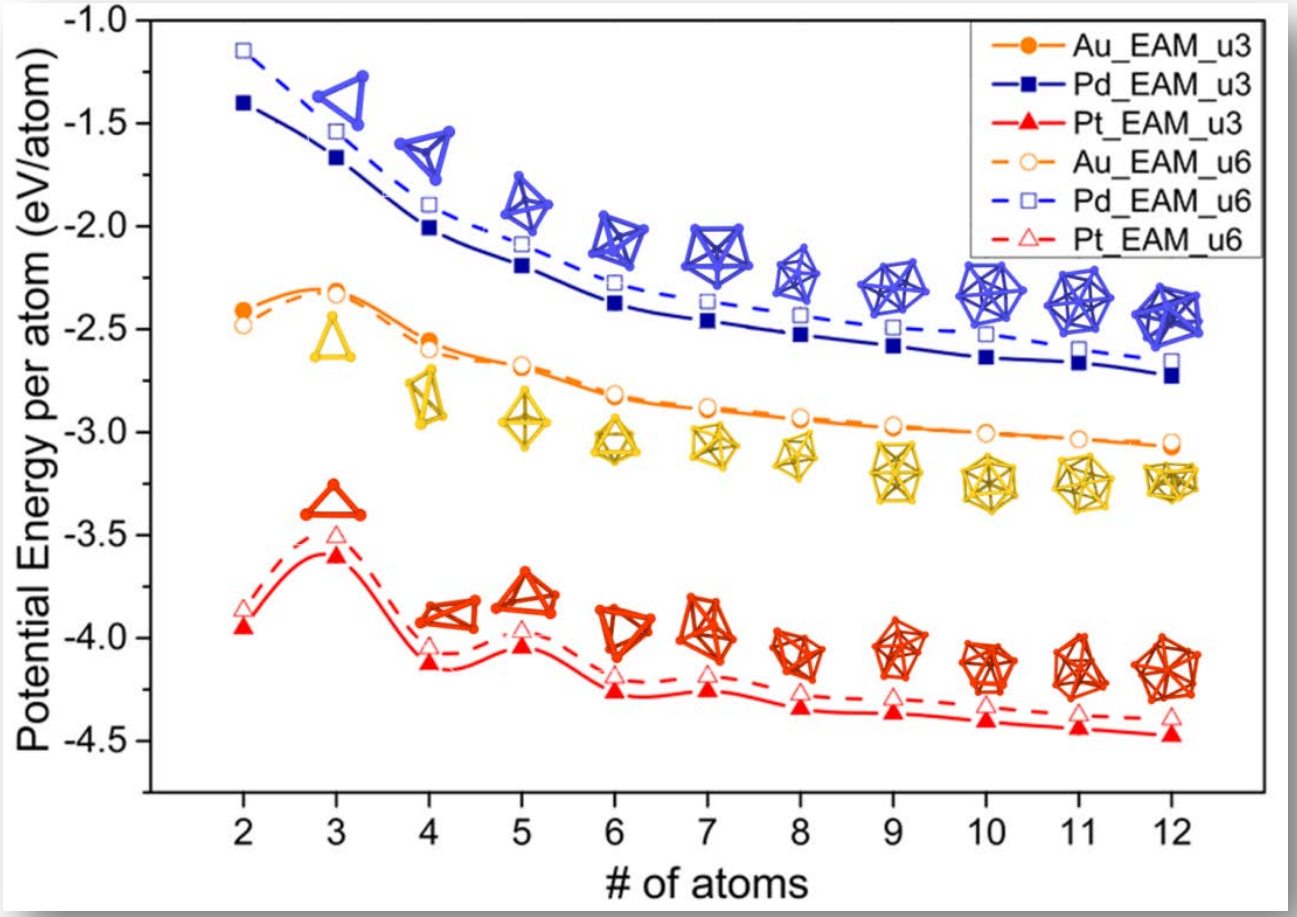

Potential energy per atom as a function of number of atoms for low nuclearity monometallic clusters

Two EAM-type potentials: Enhanced stability for Au and Pt dimers compared to trimers

Stability of Pd clusters increases monotonically with size

Mattei et al. Chem Mater, 31:6 (2019) 2151-2163

NP growth

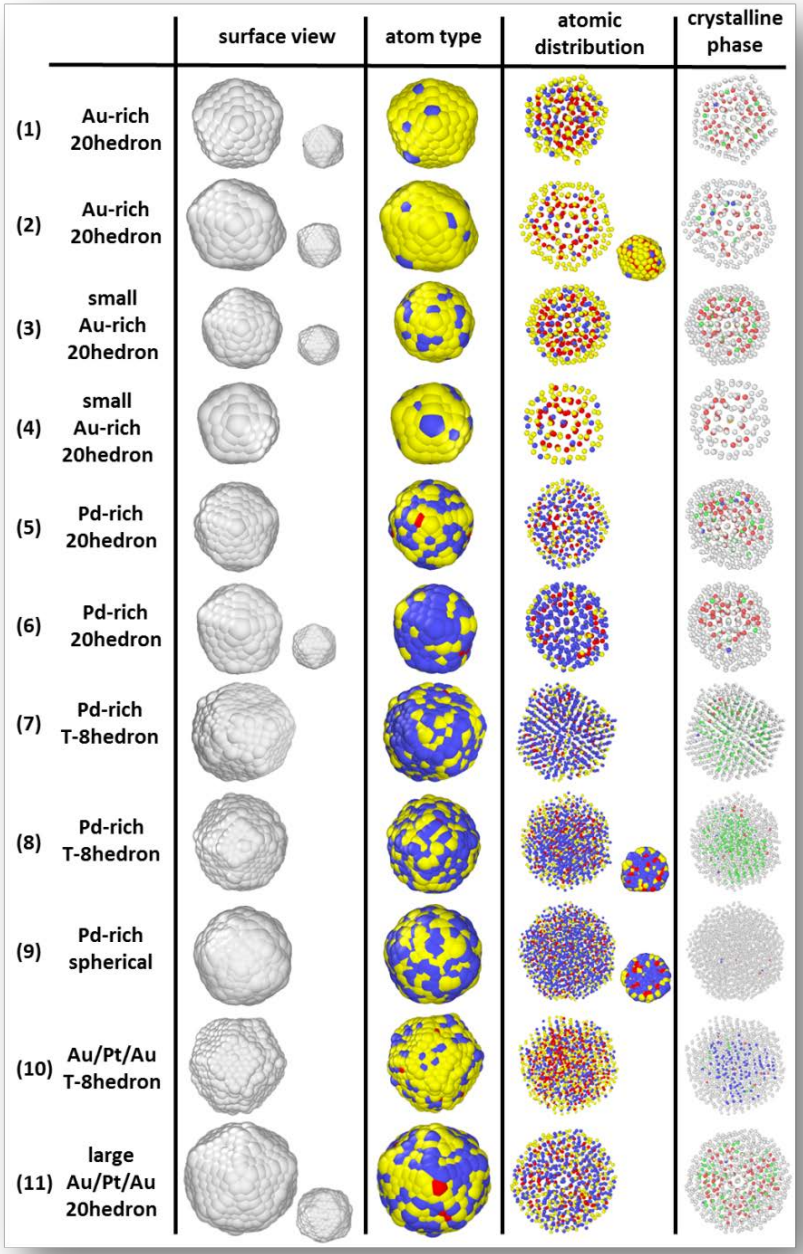

NP structures obtained by MD growth

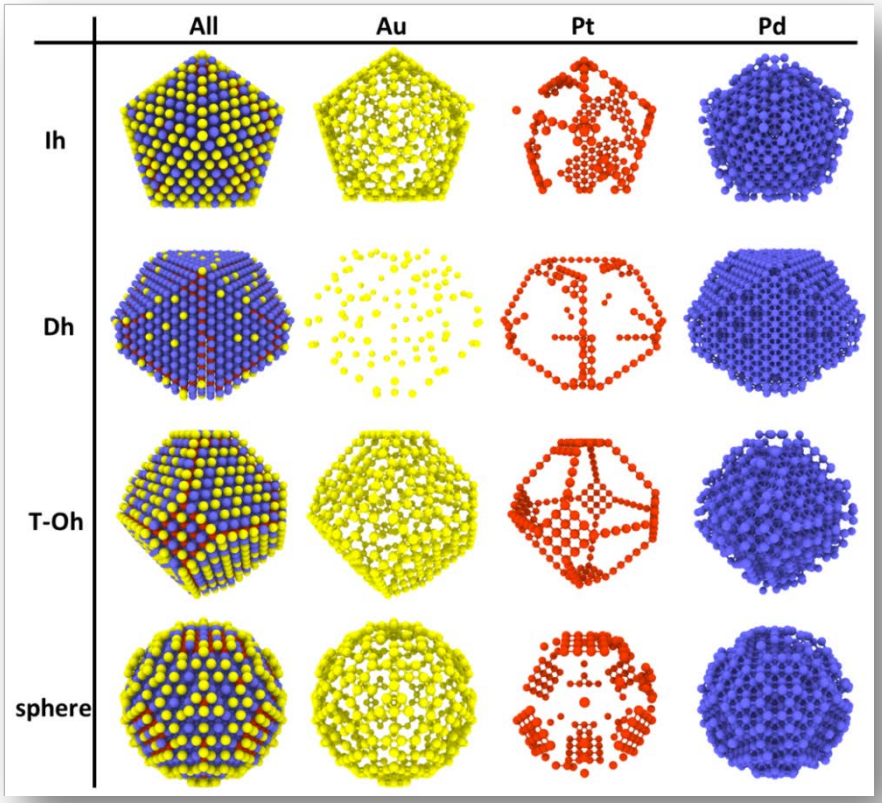

Equilibrium states of four selected geometries and compositions by MMC

Mattei et al. Chem Mater, 31:6 (2019) 2151-2163

TEM characterisation

trimetallic Pd-15 W/Au-5 W/Pt-5 W sample

Physical order:
HR-TEM micrographs

Chemical order:
STEM-HAADF micrographs

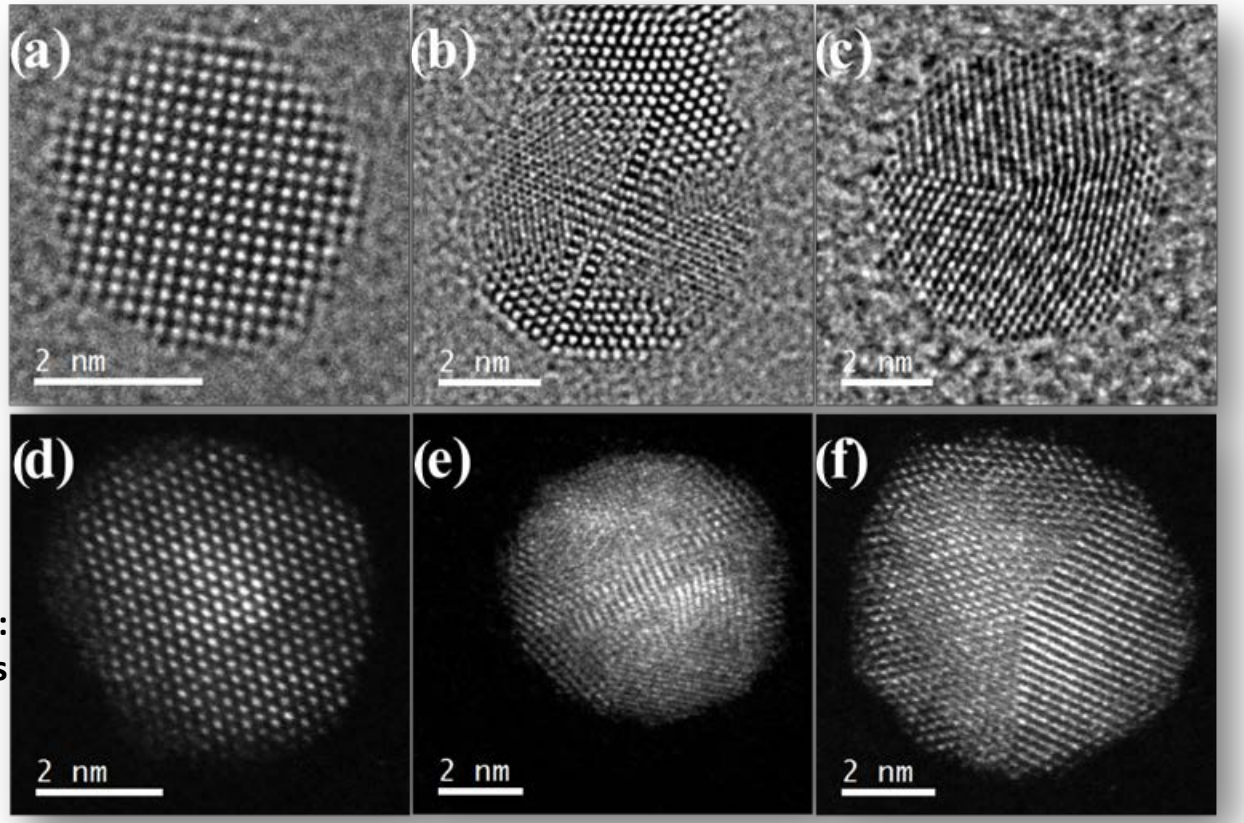

(a) fcc particle viewed along its [100] zone axis
(b) icosahedral particles viewed along their twofold symmetry axes
(c) decahedral particle viewed along its fivefold symmetry axis

(d) fcc particle viewed along its [101] zone axis
(e) Icosahedron viewed along its twofold symmetry axis
(f) fivefold twinned nanoparticle (decahedron)

Mattei et al. Chem Mater, 31:6 (2019) 2151-2163

Nanoparticle coalescence

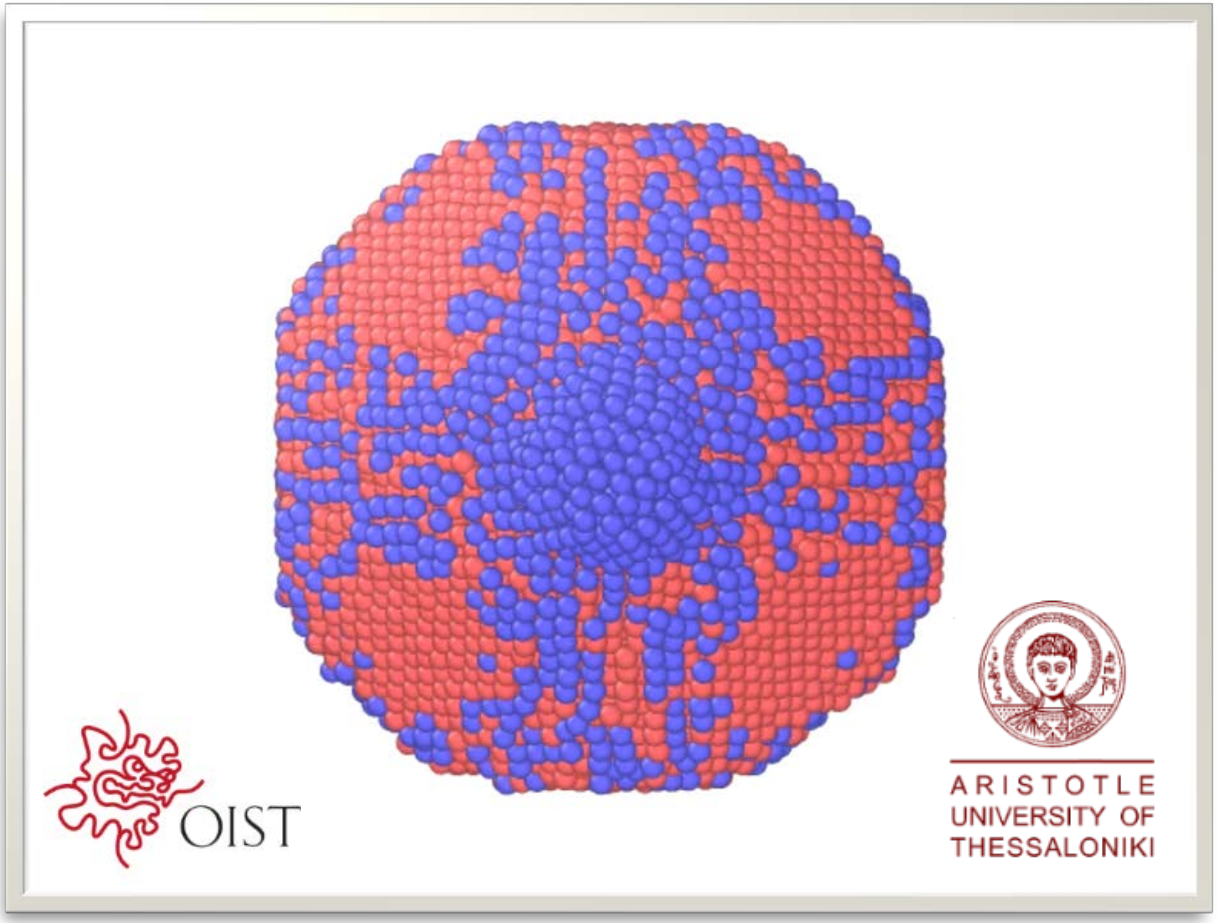

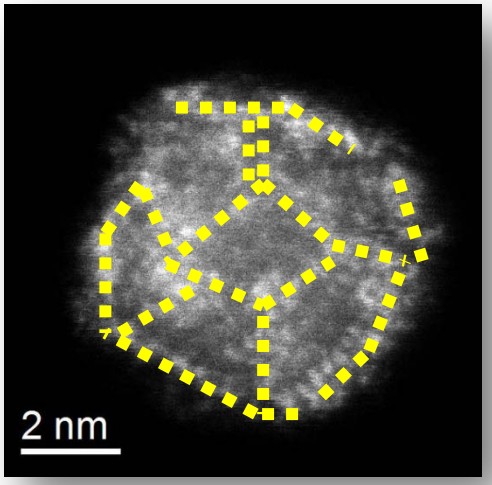

(NiPt)

Grammatikopoulos *et al.*, Kinetic trapping through coalescence and the formation of patterned Ag-Cu nanoparticles, Nanoscale 8 (2016) 9780-9790

Multiple mechanisms simultaneously at play

Overview of multi-step Fe-Au nanocube growth model

(1) Nucleation of monometallic clusters

(2) Coalescence and wetting

(3) Concurrent further deposition of residual Fe atoms in vapour phase and surface segregation of Au atoms in the nanocube create the core-frame morphology

(4) Surface diffusion of Au atoms leads to vertex and edge decoration

(5) Final multiple-frame morphology.

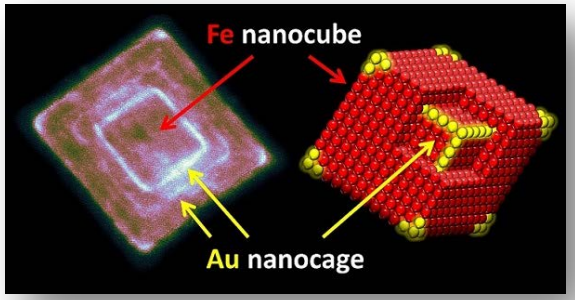

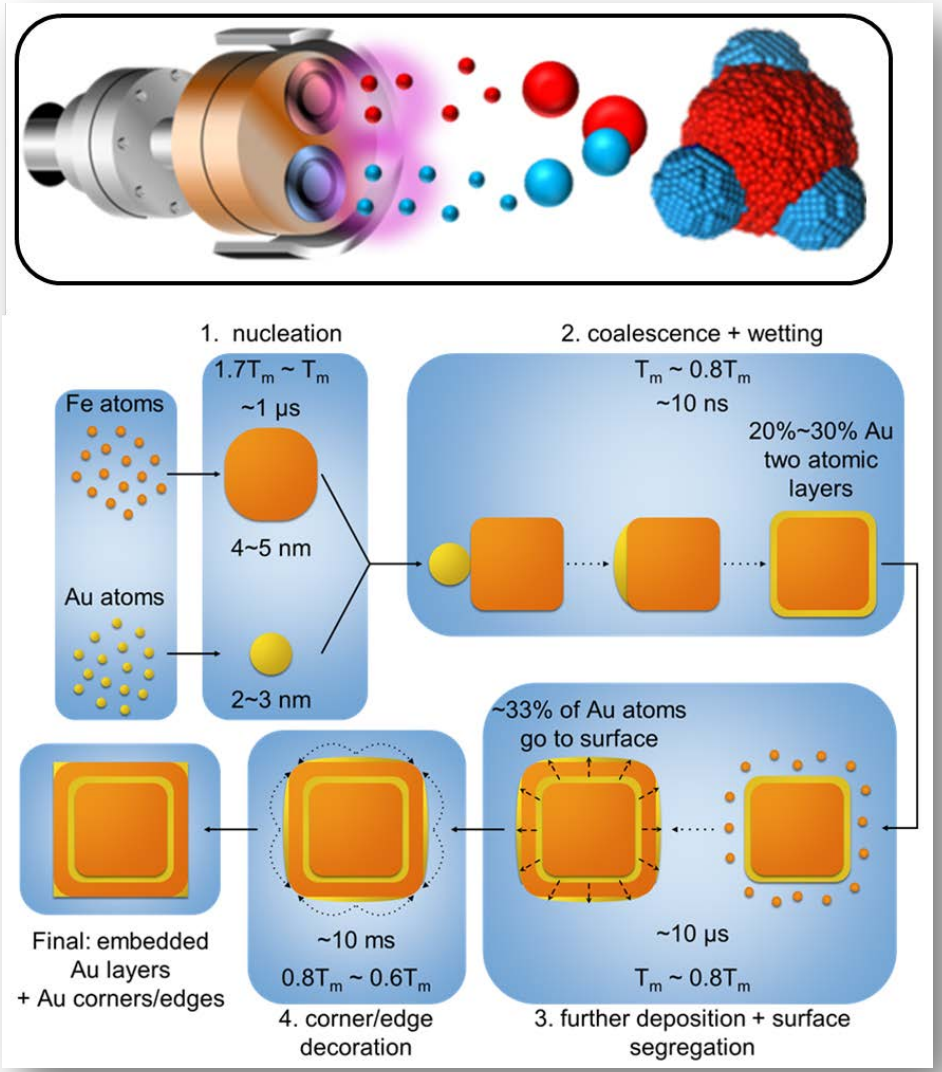

Vernieres et al. Adv Sci, 6 (2019) 1900447

From Nanoparticles by Design…

… to Design by Nanoparticles

individual atoms

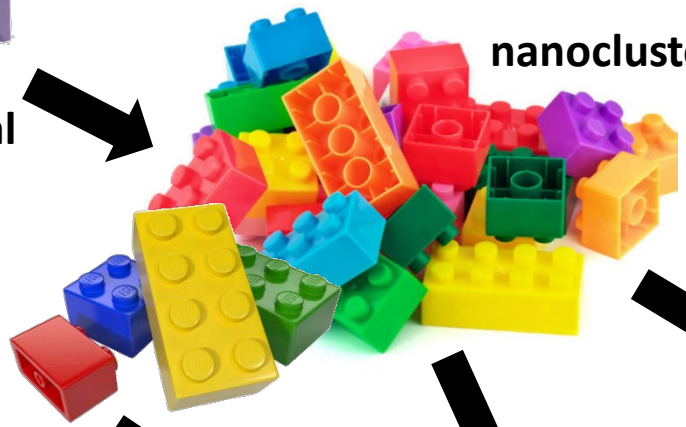

nanoclusters

cluster-surface interaction

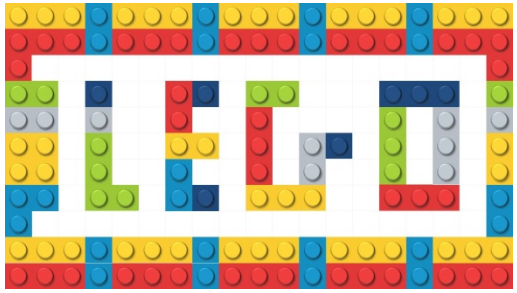

nanodevices

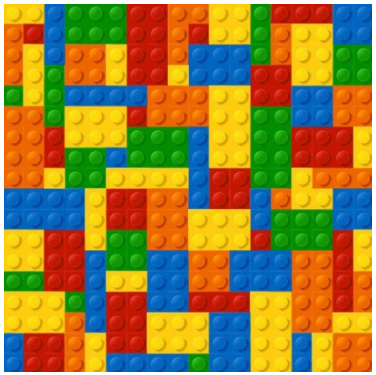

2D films

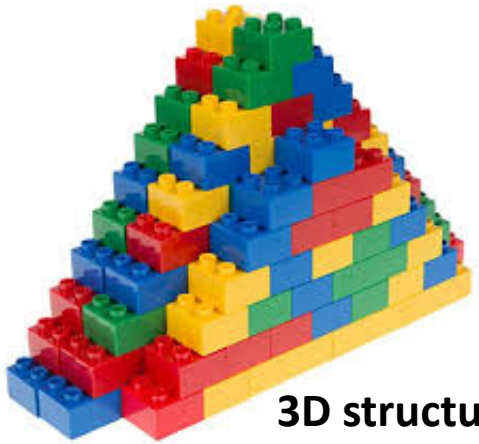

3D structures

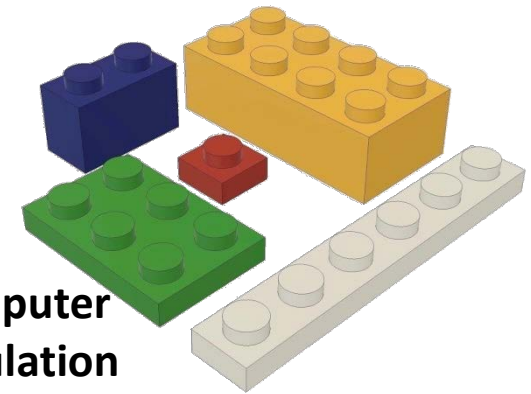

computer simulation

Nanoportals for H-storage and Electrocatalysis

- Mg is an attractive material for H storage due to its high reversible H mass capacity of 7.6 wt.%

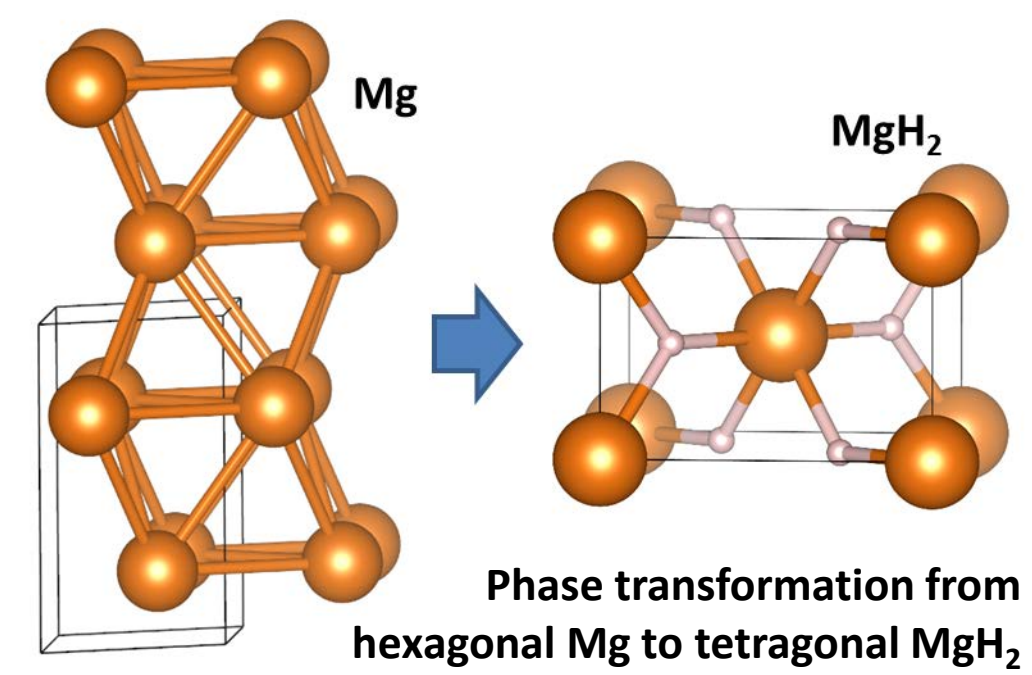

Problems

- High desorption temperature
- Slow room-temperature hydrogen sorption kinetics

Use of Pd capping layers the answer?

Pd-capped Mg nanofilms suffer from a ‘‘blocking-effect” of MgH_2 at the Pd–Mg interface:

- use of high temperatures in order to accelerate the kinetics results in Pd inter-mixing with Mg, which typically forms intermetallic compounds (Mg_5Pd_2, Mg_3Pd, Mg_6Pd)
- the Pd capping layer often delaminates after a few sorption cycles, resulting in reduced MgH_2 formation

Kumar et al. Adv En Mater, 8 (2018) 1701326

Advantages of using nanoparticles

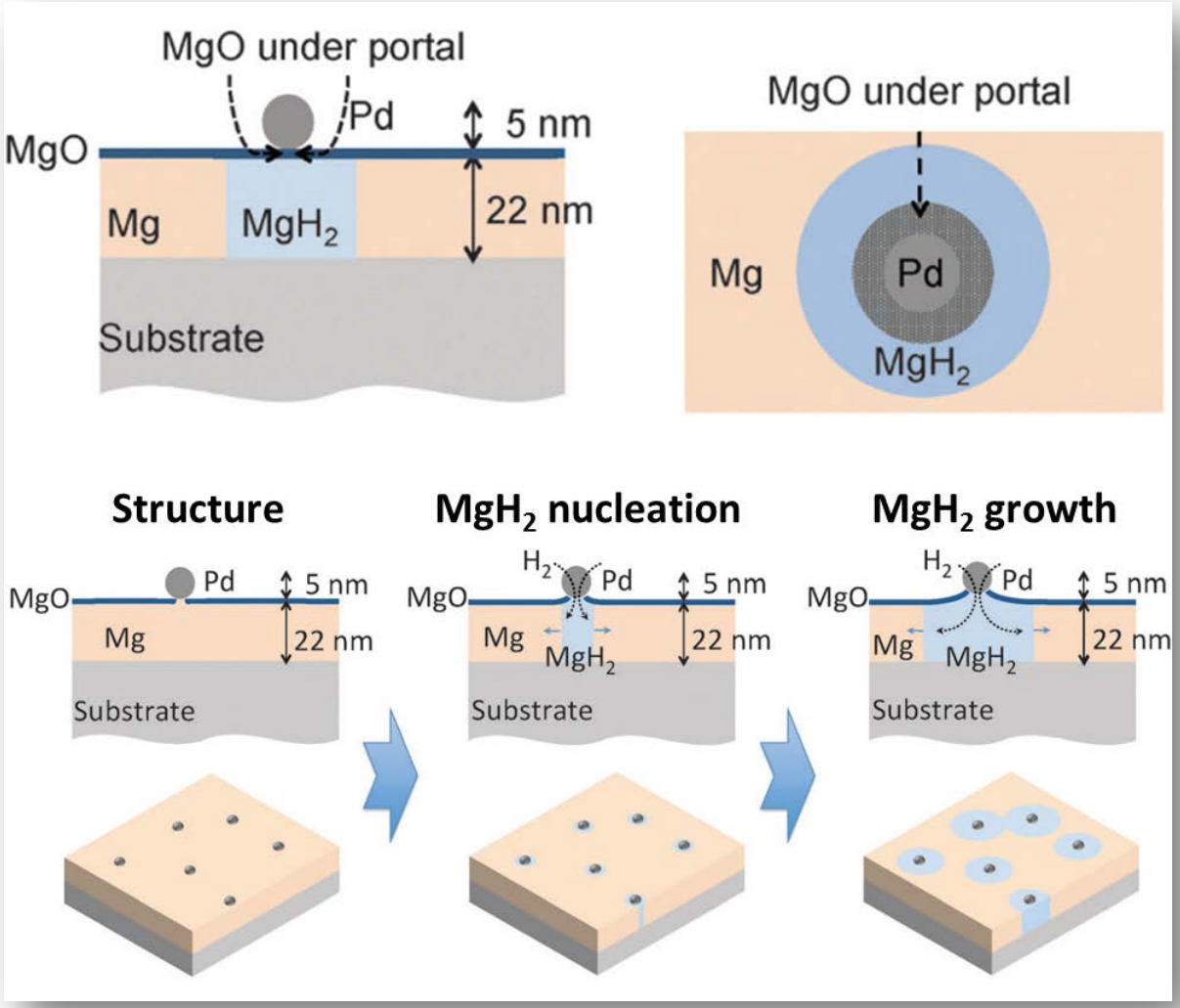

- ✓ NPs are generally well-known to exhibit enhanced catalytic activity, compared to bulk or nanofilm systems
- ✓ compressive stress and delamination can be prevented
- ✓ monodispersed Pd NPs can potentially reduce the degree of alloy formation at high temperature (less Pd in contact with Mg)
- ✓ much less material used

C.-J. Chung et al., Phys. Chem. Chem. Phys, 17(43), 2015, 28977-28984

Deposition procedure

Advantage: possibility to let oxidise

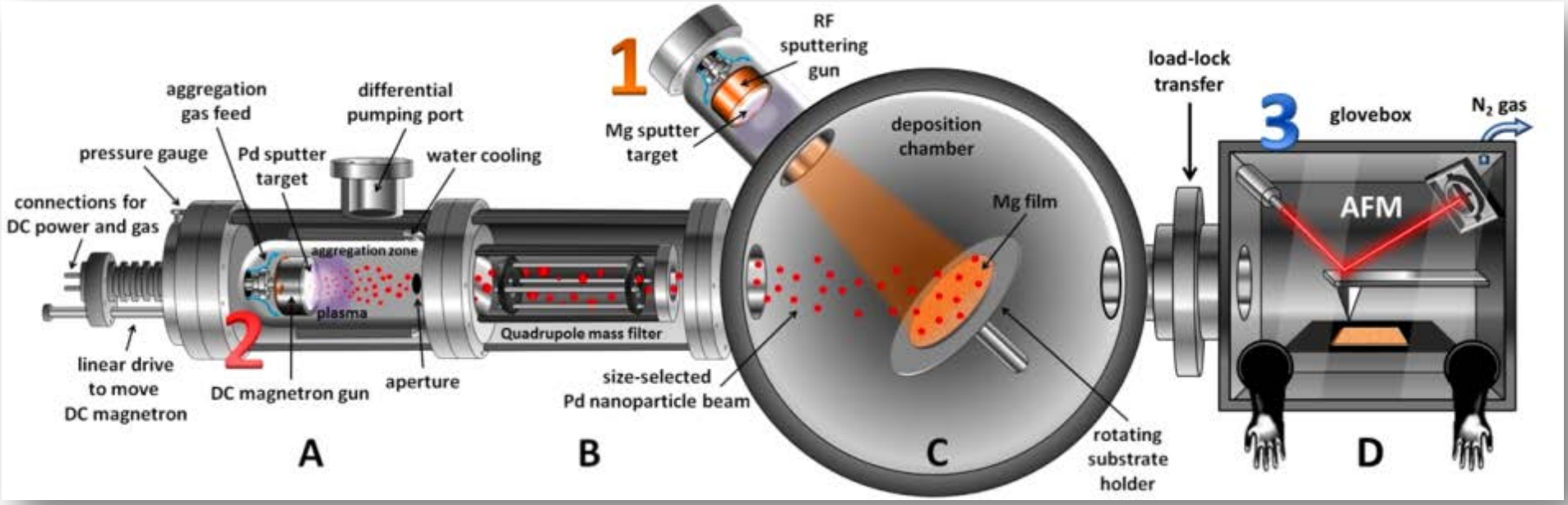

Experimental Setup

Kumar et al. Adv En Mater, 8 (2018) 1701326

Summary of mechanism

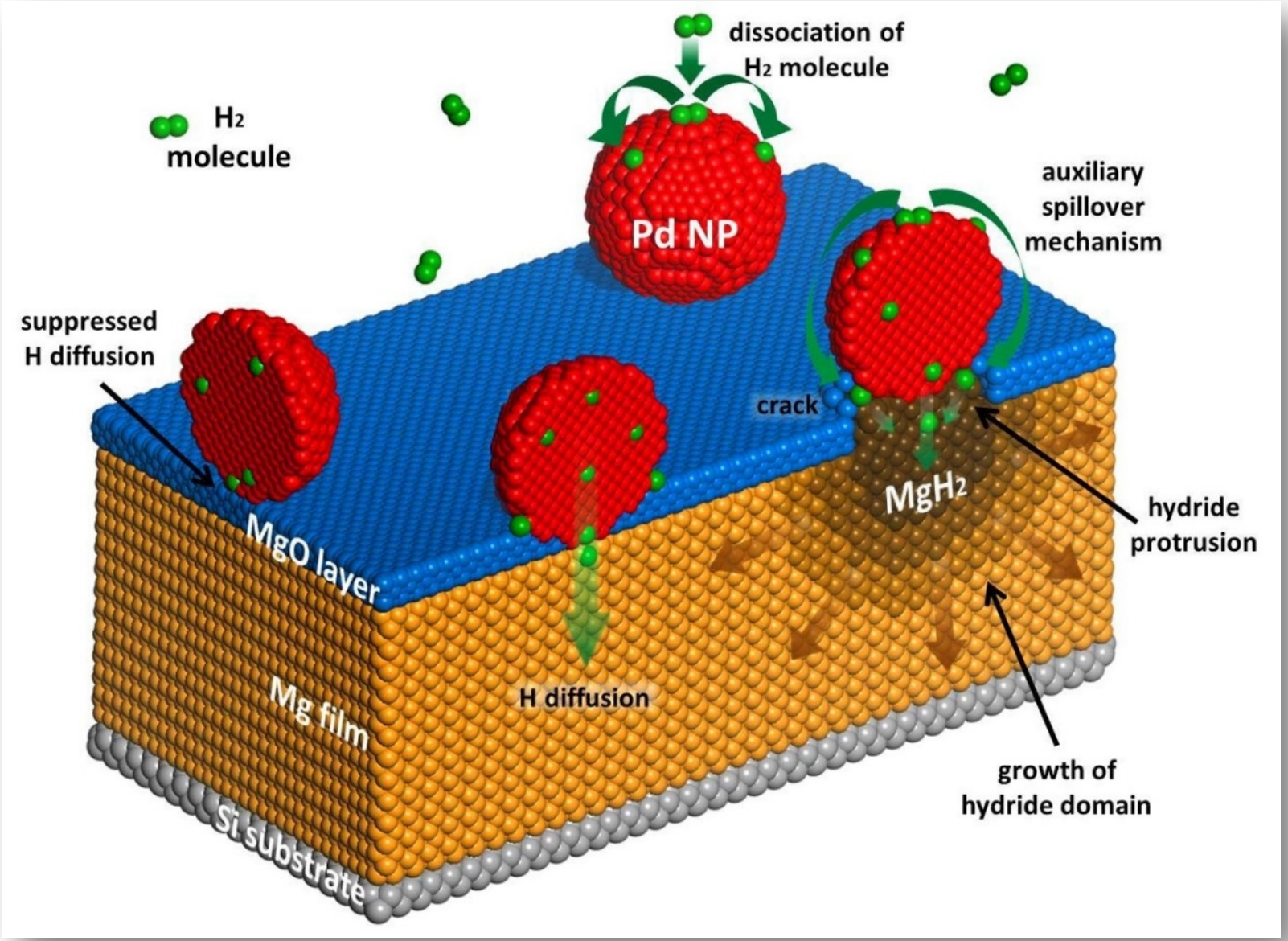

Kumar et al. Adv En Mater, 8 (2018) 1701326

Proof via DFT

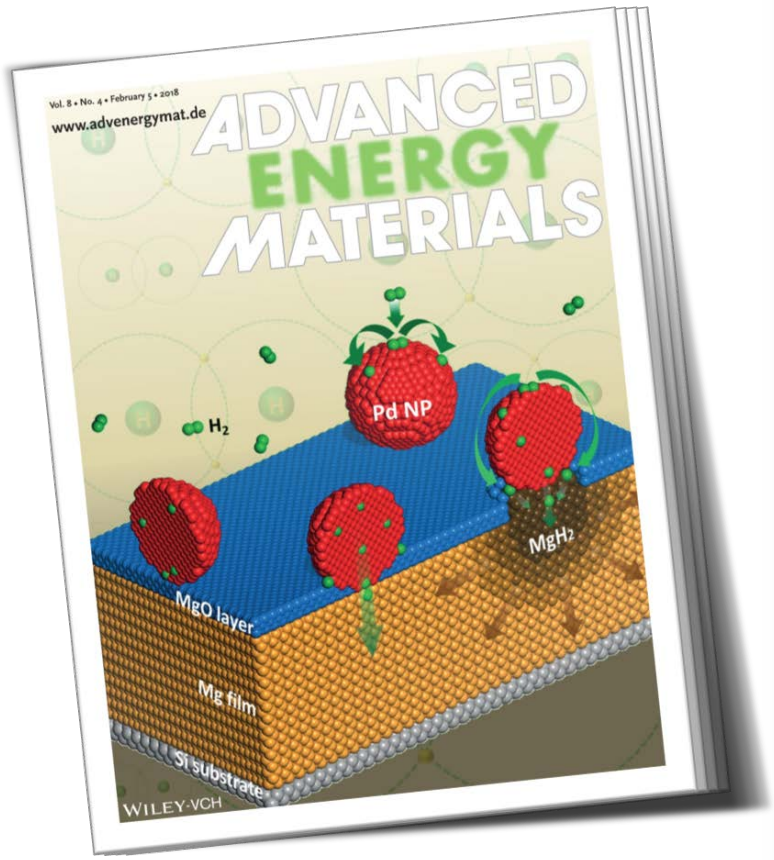

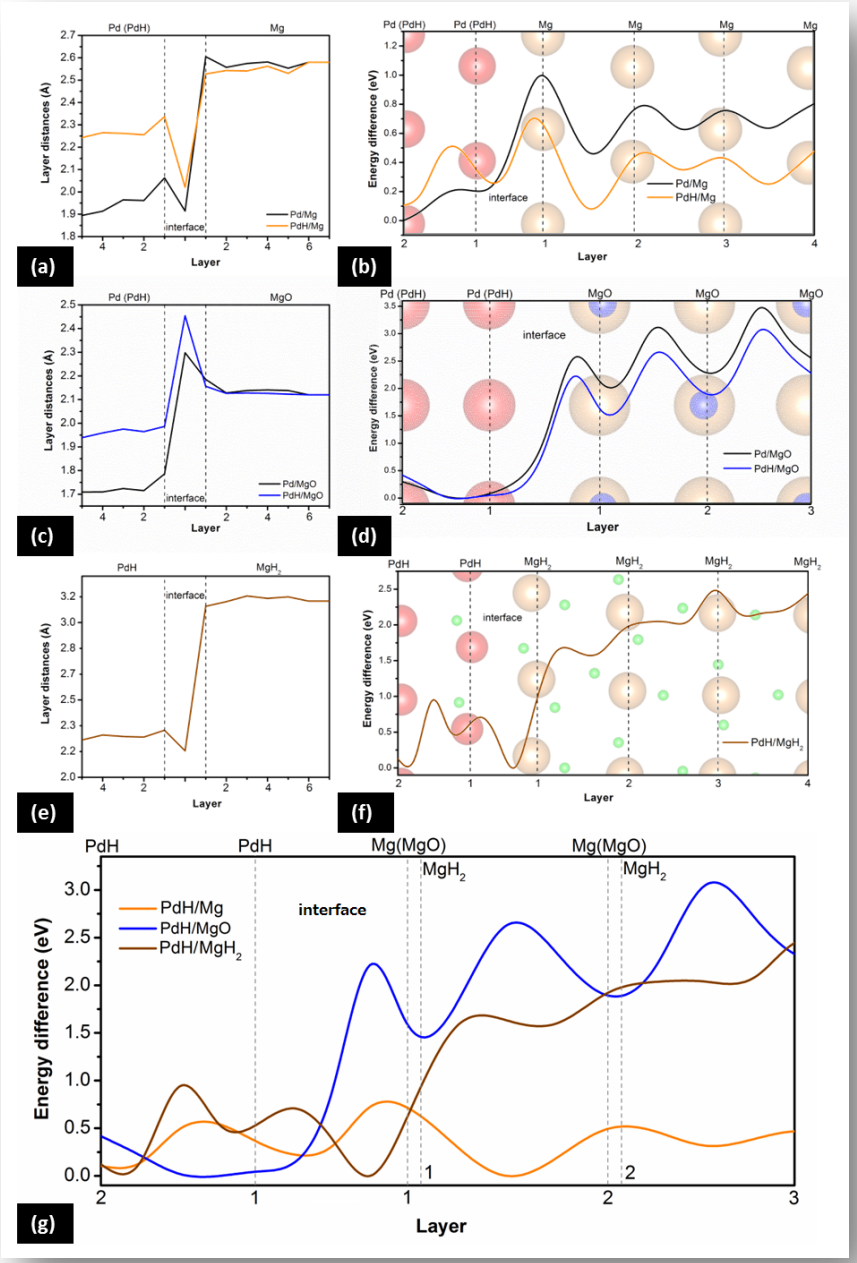

Kumar et al. Adv En Mater, 8 (2018) 1701326

Pd nanoportals for single NP electrochemistry

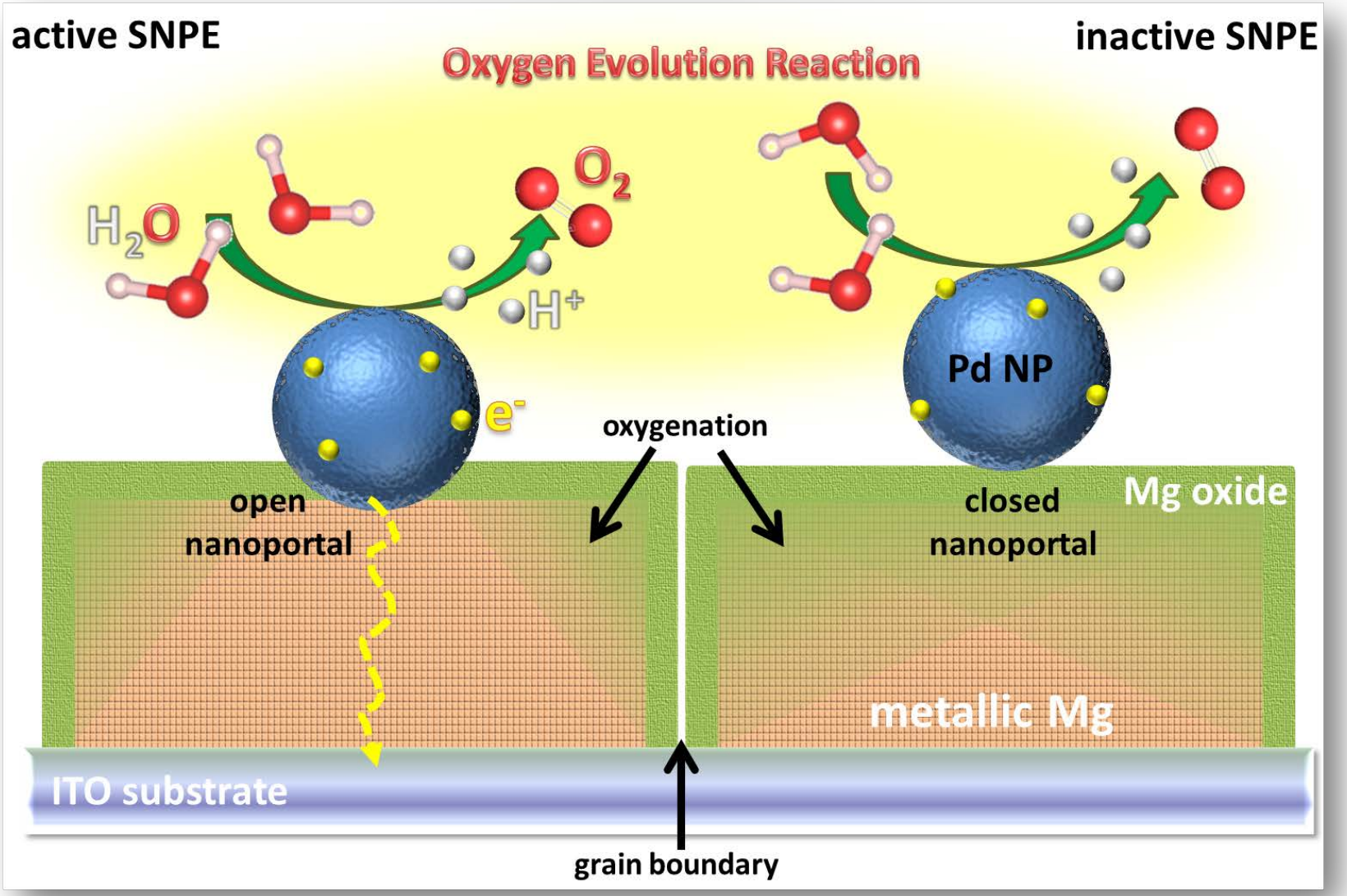

Datta et al. JPC C, 123 (2019) 26124

Pd nanoportals for single NP electrochemistry

HCP Pd NP (0001) on (0001) Mg/ (100) MgO

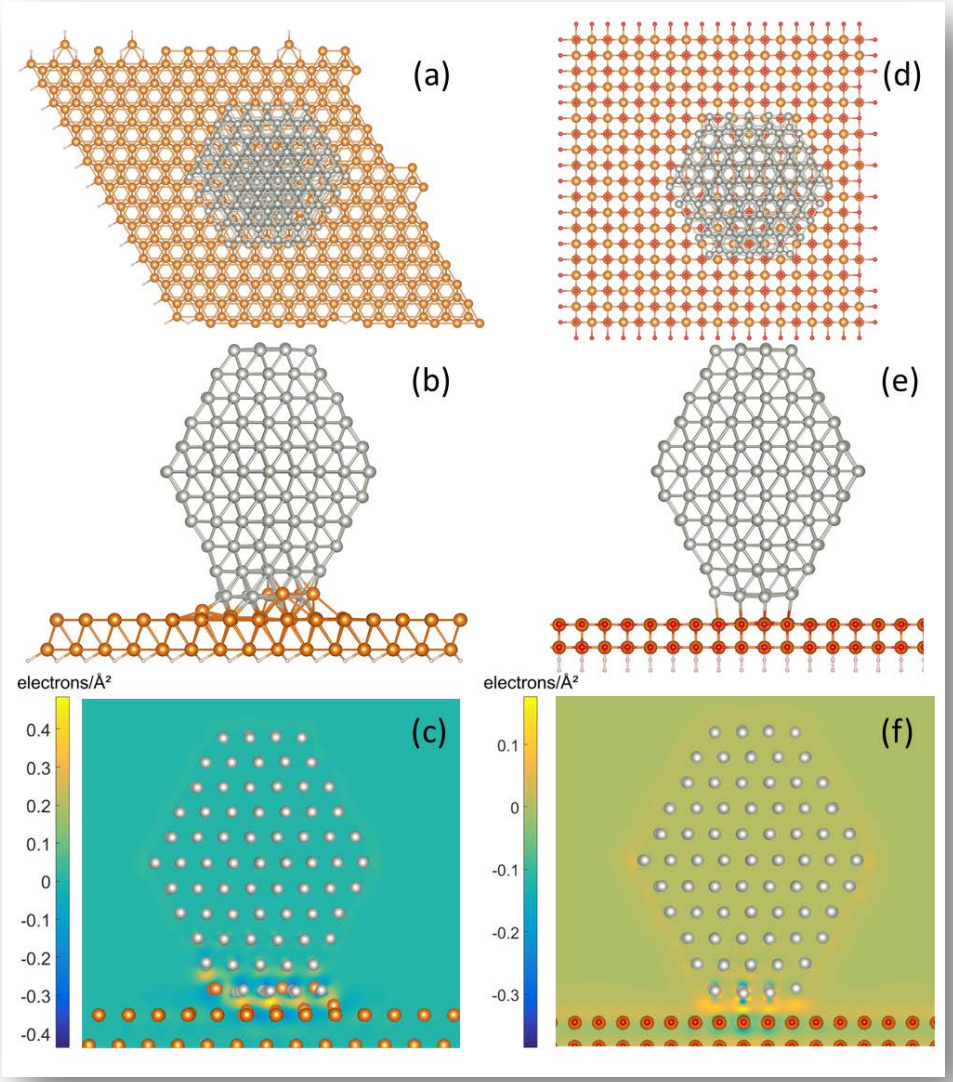

20hedral Pd NP (111) on (0001) Mg/ (100) MgO

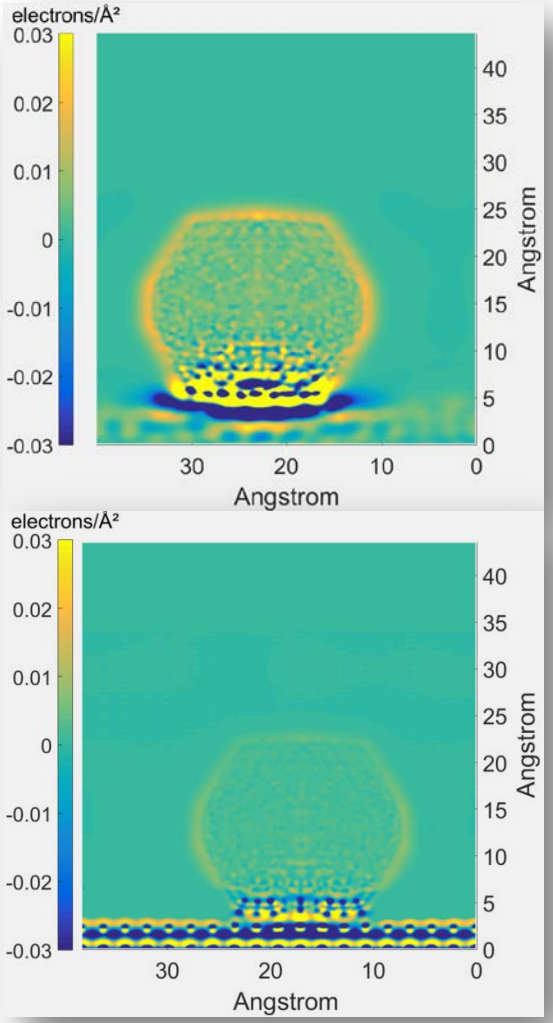

Datta et al. JPC C, 123 (2019) 26124

Thank you for your attention!